Available online at www.sciencedirect.com
ScienceDirect
Bioorganic & Medicinal Chemistry Letters 18 (2008) 1288–1292
Bioorganic & Medicinal Chemistry Letters

α,β-Cyclic-β-benzamido hydroxamic acids: Novel oxaspiro[4.4]nonane templates for the discovery of potent, selective, orally bioavailable inhibitors of tumor necrosis factor-α converting enzyme (TACE)

Gregory R. Ott,* Naoyuki Asakawa, Rui-Qin Liu, Maryanne B. Covington, Mingxin Qian, Krishna Vaddi, Robert C. Newton, James M. Trzaskos, David D. Christ, Laurine Galya, Thomas Scholz, Will Marshall and James J.-W. Duan

Departments of Discovery Chemistry and Discovery Biology, Bristol-Myers Squibb Research and Development, Rte 206 and Province Line Road, Princeton, NJ 08543, USA

Received 11 December 2007; revised 4 January 2008; accepted 8 January 2008
Available online 11 January 2008

Abstract—Two novel oxaspiro[4.4]nonane β-benzamido hydroxamic scaffolds have been synthesized in enantio- and diasteriomerically pure form. These templates proved to be exceptional platforms that have led to the discovery of potent inhibitors of TACE that are active in a cellular assay measuring suppression of LPS-induced TNF-α. Furthermore, these inhibitors are selective against related MMPs, demonstrate permeability in a Caco-2 assay, and display good oral bioavailability.

Tumor Necrosis Factor-α (TNF-α), a pro-inflammatory cytokine, has been the subject of intense interest for its purported role in numerous pathological diseases.[1] The modulation of TNF-α as a drug discovery target has been validated by the clinical success of the anti-TNF-α biologics entaneracept, infliximab, and adalimumab.[2] From the point of view of small molecule drug discovery, an alternative target to mitigate TNF-α production is the metalloprotease TNF-α converting enzyme (TACE).[3]

The search for non-peptidic inhibitors of TACE has led to the discovery of novel α,β-cyclic-β-benzamido hydroxamic acids.[4,5] These studies demonstrated that the active site tolerates a wide variety of rings including 5- and 6-membered carbocyclic and heterocyclic rings including cyclopentane, pyrrolidine, tetrahydrofuran, cyclohexane, tetrahydropyran, and piperidine systems. A representation of the binding motif of these inhibitors is shown in Fig. 1. In accordance with homology modeling, the active conformation presents the ring into solvent.[6] Interestingly, data generated from the initial carbocyclic leads indicated that for oral bioavailability, a certain degree of lipophilicity was required in the cyclic β-amino acid portion of the inhibitor, but was deleterious to obtaining the necessary cellular potency. It was demonstrated that certain cyclic β-amino acid derivatives including tetrahydropyran, tetrahydrofuran, and substituted pyrrolidine β-amino hydroxamic acids were preferred.[4,5]

During the examination of substituent effects on the 4-position of the (1*R*,2*S*)-cyclopentane-β-benzamido

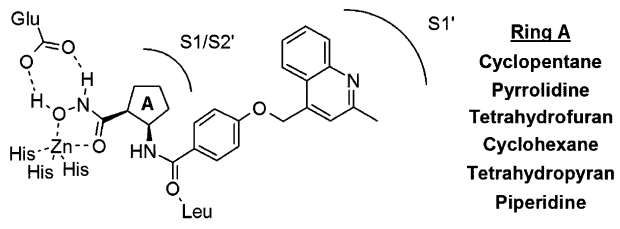

Figure 1. TACE inhibitors, *cis*-α,β-cyclic-β-amino acid scaffolds.

Keywords: TACE; TNF-α converting enzyme; MMP; Matrix metalloprotease; β-Amino acid.
* Corresponding author at present address: Cephalon, Inc. 145 Brandywine Parkway, West Chester, PA 19380, USA. Tel.: +1 610 738 6861; fax: +1 610 738 6558; e-mail: gott@cephalon.com

0960-894X/$ - see front matter © 2008 Elsevier Ltd. All rights reserved.
doi:10.1016/j.bmcl.2008.01.030

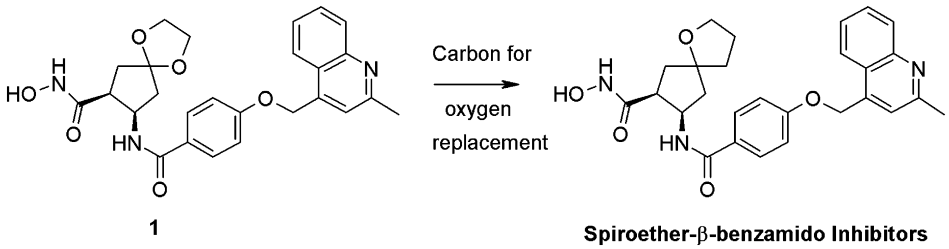

Figure 2. Design of spiroether-β-benzamido hydroxamic acid template.

hydroxamic acid scaffold,[5a] it was shown that the 1,3-dioxolane moiety (**1,** Fig. 2) is not only tolerated in the active site (pTACE IC_{50} = 1.0 nM), it imparts a dramatic boost to potency in the cellular suppression of LPS-induced TNF-α in human whole blood (WBA, IC_{50} = 24 nM), as compared to the unsubstituted parent cyclopentane (WBA IC_{50} = 475 nM).[4,7] Importantly, in vitro screening parameters predictive of oral absorption (Caco-2) illustrated that **1** had promising permeability ($P_{app} = 1.8 \times 10^{-6}$ cm/s). Unfortunately, the acid labile nature of the dioxolane precluded advancing a compound with that moiety. Furthermore, the resultant hydrolysis product (i.e. the ketone), though potent, showed poor Caco-2 permeability.[5a]

Since **1** appeared to have a desirable in vitro profile (WBA IC_{50} = 24 nM, Caco-2 $P_{app} = 1.8 \times 10^{-6}$ cm/s), we felt that the structural motif represented by the

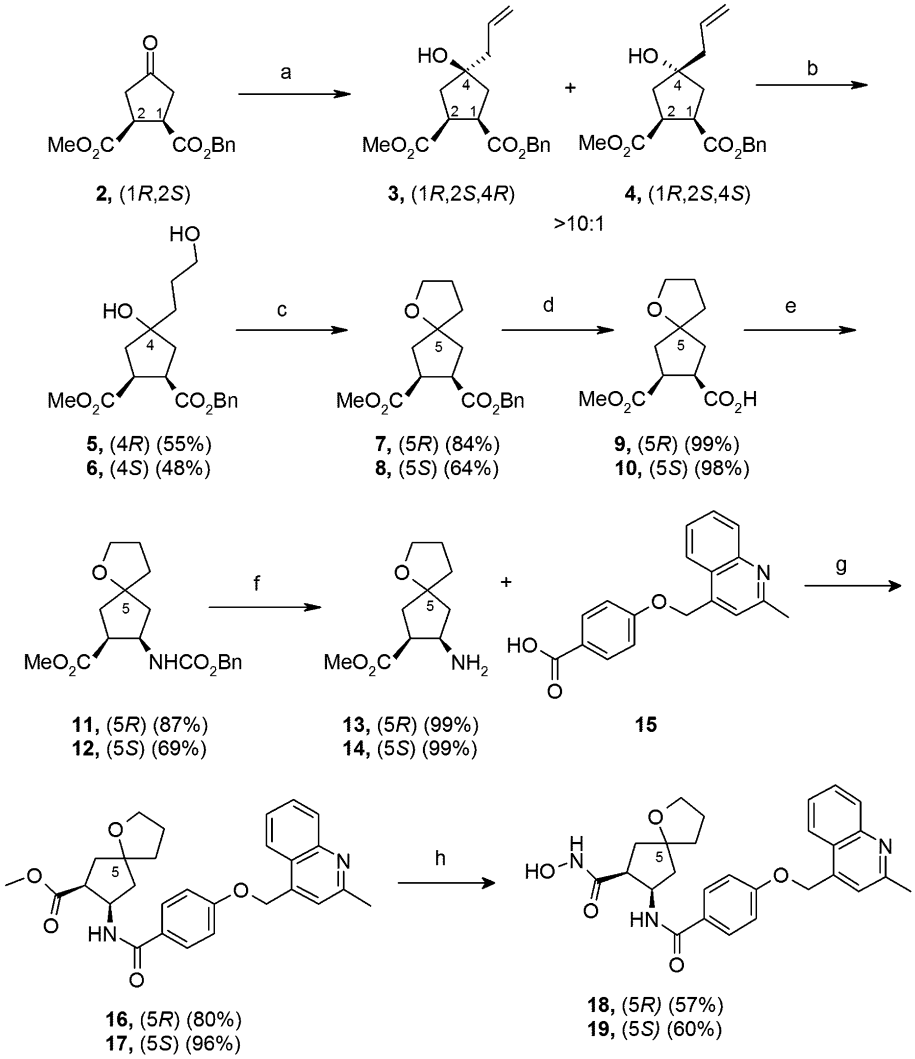

Scheme 1. Reagents and conditions: (a) Allyltrimethylsilane, $TiCl_4$, CH_2Cl_2 (57%); (b) $BH_3 \cdot THF$; NaOH, H_2O_2; (c) MsCl, TEA, CH_2Cl_2, 0 °C to reflux; (d) H_2, $Pd(OH)_2$/C, MeOH; (e) *i*-PrO_2CCl, TEA; NaN_3, H_2O; benzene, reflux; BnOH, p-TsOH, reflux; (f) H_2, $Pd(OH)_2$/C, MeOH; (g) BOP reagent, DIPEA, DMF; (h) NH_2OH, NaOMe, MeOH.

dioxolane system may be transformed into a viable alternative which would impart both the necessary polarity to achieve cellular potency and the desired lipophilicity to impart bioavailability. To exploit this unique architecture we proposed exchange of one of the oxygens of the dioxolane species with a carbon, thus revealing a novel spiroether scaffold (Fig. 2). It was expected that this oxaspiro[4.4]nonane system would retain the in vitro properties of the dioxolane system, while remaining stable to hydrolytic conditions.

Installation of the β-amino-acid portion of the inhibitor would be achieved using a Curtius rearrangement of an appropriately substituted dicarboxylate (Scheme 1).[8] The spiroether portion of the β-amino acid template was envisioned to arise from addition of an allyl nucleophile to a ketone to give a quaternary carbinol followed by hydroboration of the olefin and intramolecular ether formation. Thus, Lewis-acid catalyzed addition of allyltrimethylsilane to ketone **2**[5a,9] provided the desired allyl addition products in >10:1 ratio of (4*R*) to (4*S*). Compounds **3** and **4** were separated using silica gel chromatography and taken on independently; the structure was assigned by correlation with later products (vide infra). The olefin of the allyl group was hydroborated which provided the desired hydroxyl derivatives in modest isolated yield. The primary alcohols were mesylated, then heated at reflux to effect cyclization. The oxaspiro[4.4]nonane systems[10] **7** and **8** were isolated in good yield. Debenzylation followed by Curtius rearrangement gave the Cbz-protected amines **11** and **12**. The free amines **13** and **14** were delivered by hydrogenation. Coupling to carboxylic acid **15**[4] afforded the complete carbon skeleton of the inhibitors. Treating the esters **16** and **17** with a solution of hydroxylamine hydrochloride and sodium methoxide in methanol that had been premixed and filtered provided the inhibitors **18** and **19** in 57% and 60% isolated yields, respectively.

NMR analysis of both **18** and the phenol derivative **21** revealed the relative stereochemistry of the spiroether system. **21** was prepared by reductive cleavage of the quinolinyl moiety from **16** and conversion of the derived ester **20** to the hydroxamic acid **21** (Scheme 2).

The results from the NMR experiments are shown in Fig. 3. For **18**, nOe's were observed for H_1 to $H_{5\alpha}$ and $H_{5\alpha}$ to H_8. Furthermore, using a 2D-ROESY experiment, nOe was observed from H_1 to H_8, thus indicating that the spiroether has the (*R*)-stereochemistry. In addition, the phenol derivative **21** displayed similar nOe's from H_1 to $H_{5\alpha}$ and $H_{5\alpha}$ to H_8 using a GOESY experiment.[11]

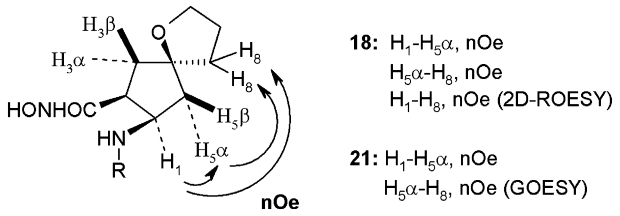

Figure 3. Observed nOe's in **18** and **21**.

The stereochemistry determined by NMR analysis was confirmed by single crystal X-ray of the phenol derivative **21**.[12] A 3-D representation of the crystal structure of **21** is shown in Fig. 4.

The independently synthesized spiroether β-amino hydroxamates **18** and **19** were tested in vitro using semi-purified porcine TACE (pTACE)[13] since there is high sequence homology between the human and porcine forms of TACE. Selectivity against matrix metallo-

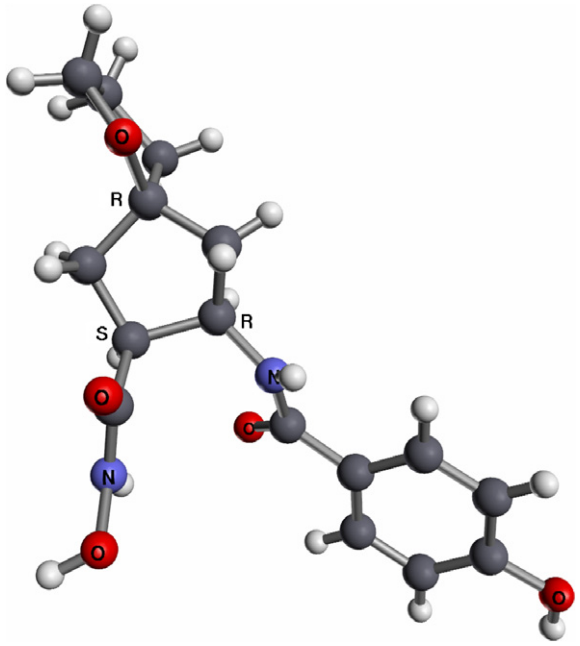

Figure 4. 3-D representation of **21** from X-ray coordinates.

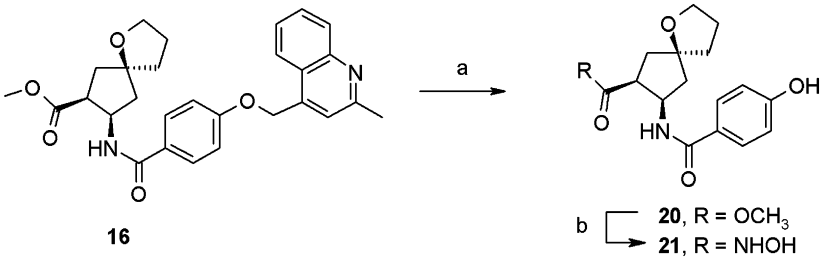

Scheme 2. Reagents: (a) Zn, AcOH, CH_2Cl_2 (83%); (b) NH_2OH, NaOMe, MeOH (55%).

proteases (MMPs) was determined using MMP-1 as a representative with a shallow S1' pocket and MMP-2 and MMP-9 with deep S1' pockets. Cellular inhibition of LPS-stimulated TNF-α was measured in human whole blood (WBA). We desired potency in a cellular assay since there is evidence that suggests proteolytic activity of TACE occurs both in an intra- as well as extracellular fashion.[14] In vivo pharmacokinetics were determined following iv and oral dosing using LC/MS/MS.[15] In vivo efficacy was determined in an acute model of endotoxemia in mouse.[13]

Shown in Table 1 are the in vitro results for **18** and **19**. Both isomers were extremely potent against pTACE (1.0 nM, respectively). Importantly, **18** and **19** displayed potency in the cellular suppression of TNF-α. As compared to the dioxolane **1**, several-fold loss in activity was observed and potency still remained in the desired range (WBA $IC_{50} < 200$ nM). Following the previously established paradigm, the 4-[(2-methylquinolin-4-yl)methoxy]benzamide P1' moiety imparted the desired selectivity;[16] **18** and **19** displayed >1000-fold selectivity for pTACE over MMP − 1, −2, and − 9. We were gratified to find that both examples gave Caco-2 values indicative of good oral absorption (i.e. $P_{app} > 1.0 \times 10^{-6}$ cm/s) with **18** demonstrating $P_{app} = 5.7 \times 10^{-6}$ cm/s and **19** having $P_{app} = 1.5 \times 10^{-6}$ cm/s. Consistent with the Caco-2 values, both **18** and **19** proved to be orally bioavailable in Sprague–Dawley rats.

Shown in Table 2 are the pharmacokinetic profiles of **18** and **19** after iv (5 mg/kg) and oral dosing (5 mg/kg) in Sprague–Dawley rats. Data obtained for **18** and **19** were obtained from n-in-1 cassette dosing studies. Both **18** and **19** displayed low clearance following iv dosing (0.7 and 0.8 L/h/kg, respectively). **18** had a much smaller volume of distribution (0.3 L/kg) as compared to **19** (1.4 L/kg). The iv half-life for **18** was 4.2 h and for **19** was 6.9 h. The overall iv exposure for each compound was quite high as measured by the total AUC, 12,628 nMh for **18** and 10,947 nMh for **19**. After oral administration, both compounds were rapidly absorbed with $t_{max} = 0.1$ and 0.25 h for **18** and **19**, respectively. The oral half-lives were also quite similar, for **18** (1.3 h) and **19** (1.9 h). The oral exposure as measured by AUC was 3930 nMh for **18** and 3848 nMh for **19**. Oral bioavailability proved to be 31% for **18** and 35% for **19**. The overall oral pharmacokinetic profiles for the two diastereomeric inhibitors were remarkably alike. Furthermore, **18** displayed oral bioavailability in beagle dogs ($F = 68\%$).

Table 2. Pharmacokinetic parameters of **18** and **19**[a,b]

	PK parameters	**18**	**19**
IV	dose (mg/kg)	5.0	5.0
	$t_{1/2}$ (h)	4.2	6.9
	Cl (L/h/kg)	0.7	0.8
	V_{ss} (L/kg)	0.3	1.4
	AUC (nM•h)	12,628	10,947
PO	dose (mg/kg)	5.0	5.0
	t_{max} (h)	0.1	0.25
	$t_{1/2}$ (h)	1.3	1.9
	AUC (nM•h)	3930	3848
	F%	31	35

[a] Determination of 3 for each dosing group, avg. value.
[b] Data from n-in-1 cassette dosing in Sprague–Dawley rats.

Since the overall PK profiles were similar and the in vitro potencies were also comparable, **18**, available in larger quantities since it was derived from major diastereomer of the allyl addition, was analyzed for efficacy in a murine model of endotoxemia.[13] Lipopolysaccharide was administered along with different doses of **18** by oral gavage administration at $t = 0$ h. One hour post dose, the mice were euthanized, whole blood collected by cardiac puncture, and the plasma used for the measurement of TNF-α concentration. **18** displayed a dose dependent suppression of TNF-α with a calculated ED_{50} of between 1 and 3 mg/kg.

In summary, two novel oxaspiro[4.4]nonane β-benzamido hydroxamic scaffolds have been synthesized. These novel β-amino acid derivatives proved to be exceptional

Table 1. In vitro properties of inhibitors **1**, **18** and **19**

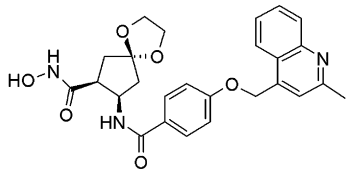

1

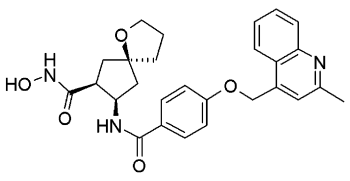

18

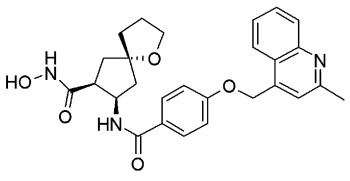

19

Compound	pTACE[a] (IC_{50}, nM)	WBA[b] (IC_{50}, nM)	MMP-1 K_i (nM)	MMP-2 K_i (nM)	MMP-9 K_i (nM)	Caco-2[c]	F% rat	F% dog
1	1.0	24	>4948	2800	>2128	1.8	—[d]	—
18	1.0	108	>4948	1357	1447	5.7	31%	68%
19	1.0	143	>4948	1920	1246	1.5	35%	—

[a] pTACE IC_{50} and MMP K_i values are from single determination.
[b] Inhibition of TNF-α release in WBA was determined with three donors.
[c] P_{app} (A → B) $\times 10^{-6}$ cm/s.
[d] —, Not determined.

platforms that, in conjunction with an optimized P1' group, have led to the discovery of potent inhibitors of pTACE. Inhibitors **18** and **19** are active in a cellular assay measuring suppression of LPS-induced TNF-α. These inhibitors are selective against MMPs and displayed good oral bioavailability in rats. Furthermore, **18** showed excellent oral bioavailability in beagle dogs. In a rodent model of endotoxemia, **18** displayed an oral ED_{50} of 1–3 mg/kg in the suppression of TNF-α.

Acknowledgment

We thank John Giannaras, Sherrill Nurnberg, and Paul Strzemienski for running in vitro assays, Robert J. Collins for LPS study in animals, Bernice Brogdon, Bing Lu, Hang Zheng, and Jingtao Wu for assistance in pharmacokinetic studies, Maria Ribadeneira for Caco-2 assay, and Gerry Everlof for running stability screens. We also thank Mary Malley for help in the preparation of Fig. 4.

References and notes

1. Newton, R. C.; Decicco, C. P. *J. Med. Chem.* **1999**, *42*, 2295.
2. (a) Moreland, L. W.; Baumgartner, S. W.; Schiff, M. H.; Tindall, E. A.; Fleischmann, R. M.; Weaver, A. L.; Ettlinger, R. E.; Cohen, S.; Koopman, W. J.; Mohler, K.; Widmer, M. B.; Blosch, C. M. *N. Engl. J. Med.* **1997**, *337*, 141; (b) Lipsky, P. E.; van der Heijde, D. M. F. M. E.; St. Clair, W.; Furst, D. E.; Breedveld, F. C.; Kalden, J. R.; Smolen, J. S.; Weisman, M.; Emery, P.; Feldmann, M.; Harriman, G. R.; Maini, R. N. *N. Engl. J. Med.* **2000**, *343*, 1594; (c) Machold, K. P.; Smolen, J. S. *Exp. Opin. Bio. Ther.* **2003**, *3*, 351.
3. For a recent review, see: Skotnicki, J. S.; Levin, J. I. *Ann. Rep. Med. Chem.* **2003**, *38*, 153.
4. Duan, J. J.-W.; Chen, L.; Lu, Z.; Xue, C.-B.; Liu, R.-Q.; Covington, M. B.; Qian, M.; Wasserman, Z. R.; Vaddi, K.; Christ, D. D.; Trzaskos, J. M.; Newton, R. C.; Decicco, C. P. *Bioorg. Med. Chem. Lett.* **2008**, *18*, 241.
5. (a) Ott, G. R.; Asakawa, N.; Lu, Z.; Liu, R.-Q.; Covington, M. B.; Vaddi, K.; Qian, M.; Newton, R. C.; Traskos, J. M.; Christ, D. D.; Decicco, C. P.; Duan, J. J.-W. *Bioorg. Med. Chem. Lett.* **2008**, *18*, 694; (b) Chen, X.-T.; Ghavimi, B.; Corbett, R. L.; Xue, C.-B.; Liu, R.-Q.; Covington, M. B.; Qian, M.; Vaddi, K. G.; Christ, D. D.; Hartman, K. D.; Ribadeneira, M. D.; Trzaskos, J. M.; Newton, R. C.; Decicco, C. P.; Duan, J. J.-W. *Bioorg. Med. Chem. Lett.* **2007**, *17*, 1865.
6. Wasserman, Z. R.; Duan, J. J.-W.; Voss, M. E.; Xue, C.-B.; Cherney, R. J.; Nelson, D. J.; Hardman, K. D.; Decicco, C. P. *Chem. Biol.* **2003**, *10*, 215.
7. Consistent with the observed paradigm that increased polarity drives cell potency, the dithiolane congener of **1**, though displaying equipotent activity in the enzymatic assay and similar MMP selectivity, does not impart a similar boost to cellular potency (WBA IC_{50} = 263 nM).
8. For examples of the preparation of cyclic β-amino acids using a Curtius rearrangement, see: Bolm, C.; Schiffers, I.; Atodiresei, I.; Hackenberger, C. P. R. *Tetrahedron: Asymmetry* **2003**, *14*, 3455.
9. All new compounds were consistent with ^{1}H NMR and low resolution mass spectrometry data.
10. The numbering system of the oxaspiro[4.4]nonane system is reflected in the structure.
11. The GOESY is a double-PFG-spin-echo, transient nOe experiment using shape selective pulses and pulse field gradients in which the results appear similar to a steady-state nOe difference experiment. Since excitation is done with shaped pulses, a much narrower region of the spectrum is affected so it is possible to see weaker nOes than with a steady-state nOe difference experiment, see Stott, K.; Keeler, J.; Van, Q. N.; Shaka, A. J. *J. Magn. Reson.* **1997**, *125*, 302.
12. The coordinates for **21** have been placed in the Cambridge Crystallographic Data Centre, deposition number: CCDC 670062.
13. Details of the pTACE (porcine TACE), MMPs, human whole blood assay (WBA) as well as LPS-mouse efficacy model are reported in previous publication, see: Xue, C.-B.; Voss, M. E.; Nelson, D. J.; Duan, J. J.-W.; Cherney, R. J.; Jacobson, I. C.; He, X.; Roderick, J.; Chen, L.; Corbett, R. L.; Wang, L.; Meyer, D. T.; Kennedy, K.; DeGrado, W. F.; Hardman, K. D.; Teleha, C. A.; Jaffee, B. D.; Liu, R.-Q.; Copeland, R. A.; Covington, M. B.; Christ, D. D.; Trzaskos, J. M.; Newton, R. C.; Magolda, R. L.; Wexler, R. R.; Decicco, C. P. *J. Med. Chem* **2001**, *44*, 2636.
14. (a) Schlondorff, J.; Becherer, J. D.; Blobel, C. P. *Biochem. J.* **2000**, *347*, 131; (b) Solomon, K. A.; Covington, M. B.; Decicco, C. P.; Newton, R. C. *J. Immunol.* **1997**, *159*, 4524.
15. Wu, J.-T.; Zeng, H.; Qian, M.; Brogdon, B. L.; Unger, S. E. *Anal. Chem.* **2000**, *72*, 61.
16. For related analogs in the α,β-cyclic-β-benzamido hydroxamic acid series, replacement of the 4-[(2-methylquinolin-4-yl)methoxy]benzamide P1' substituent with 4-[(2,6-dimethylpyridin-4-yl)methoxy]benzamide resulted in maintenance of pTACE activity but loss in both WBA activity and selectivity against MMPs-2 and -13. Ott, G. R.; Asakawa, N, unpublished results.